

APPLICATION OF NUCLEAR REACTION THEORY FOR NUCLEAR DATA EVALUATION

Mario Uhl

Institut für Radiumforschung und Kernphysik, Universität Wien
Boltzmannngasse 3, A1090 Wien, Austria

Abstract : In the past years nuclear reaction model calculations have been increasingly used in nuclear data evaluation. A brief review is given on recent developments of applied interest in the field of models and their parametrisation. The following models are considered: the optical model, the compound nucleus model, direct reaction models and phenomenological preequilibrium models.

(Nuclear reaction theory, model parameters, nuclear data evaluation,
model codes)

Introduction

The nuclear cross section data required for scientific, medical and technological applications cover a variety of different reactions in a very broad mass- and energy range. Evaluated nuclear data files as ENDF, JENDL, EFF or BROND contain a tremendous amount of numbers. It would take much time and money to measure all the cross sections given in such a file. Moreover there are many reactions of interest which are inaccessible to experiment. Therefore model calculations performed with appropriate computer codes became an indispensable tool of nuclear data evaluation. A notable advantage of cross section data generated in this way is the guarantee of flux- and energy conservation.

The employed models are based on nuclear reaction theory. Because of the complexity of the nuclear many body problem realistic models may be quite involved. On the other hand, models for massproduction of cross sections by routine calculations should be rather simple, i.e. they should be moderate in computation time requirements and, if possible, easy to handle. This demand calls for a strong interaction between basic and applied physics communities.

Simple models - and to a lesser extent also complicated ones - depend on model parameters which cannot be calculated from first principles but must be extracted from carefully selected experimental data; most of these are cross sections. In this sense model calculations can be regarded as inter- or extrapolations of experimental data and thus cannot replace measurements at all. On the contrary, by improving and extending the experimental data base the predictive power of model calculations can be increased. The availability of a carefully selected data base and, on the other side, the demand to simultaneously reproduce cross sections for many different exit channels should also be of interest for theoreticians and stimulate the collaboration with evaluators.

In this contribution I review recent progress in some reaction models and their parametrisations. Due to limitations in time I will restrict myself to the optical model, the statistical compound nucleus model, direct reaction models and phenomenological models for preequilibrium decay. The selection is of course very subjective. I omit topics which are treated in other contributions in this conference and above all those I am completely unfamiliar with.

The Optical Model

The most important ingredient of all model calculations is the optical model. First of all, this model defines the shape elastic-, the absorption- and for neutrons also the total cross section. Moreover, optical model potentials (OMP's) are required also to supply transmission coefficients for compound- and precompound models and to generate distorted waves for direct reaction models. Thus, nearly all models employed in nuclear data evaluations require OMP's in a range extending from small energies up to 20 MeV or even 100 MeV. Of course, the evaluator would prefer to use for each light particle one phenomenological optical model potential (POMP). Unfortunately the situation is not that simple. As illustrated below in the case of neutrons, the results obtained with such "global" POMP's are often not accurate enough.

In a review presented at a NEA specialist's meeting Young/1/ investigated the applicability of many global POMP's for neutrons. Most of them are derived from a spherical nuclei data base in the frame of the "single channel optical model". Therefore, when applied to permanently deformed nuclei which due to strong coupling

between elastic and inelastic channels require coupled channels calculations, the results are not satisfactory. Hence "regional" potentials for deformed nuclei were developed. However, global neutron potentials encounter also difficulties for spherical nuclei, in particular at incident energies below 10 MeV. Note that two of the most recent and most successful global neutron POMP's by Rapaport et al./2/ and by Walter and Guss/3/ are defined for $E = 7-26$ MeV and $E = 10-80$ MeV, respectively, and thus do not cover the low energy region. At the same meeting Smith et al./4/ pointed out two problems which showed up in recent work of the Argonne group. Firstly, for targets with $A = 50-130$ and energies $E = 1.5-4.0$ MeV the depth of the empirical imaginary potential exhibits a strong dependence on the mass number. Secondly, for structural materials ($A = 50-60$) it is very difficult to reproduce experimental data for $E < 5$ MeV with energy independent geometry parameters, even if coupling to the most important collective states is accounted for. The need to use energy dependent geometry parameters at low energies was reported also for other mass regions (see e.g. Refs. 5-8). Both features are not considered in commonly used global POMP's. Nevertheless, global POMP's are extremely important for cross section assessments. An investigation of global neutron POMP's is presented in this conference by Yamakoshi.

Accurate evaluations often require regional or even specific potentials which must be found by fits to appropriate experimental data. A very efficient procedure for a neutron POMP is the "SPRT" method developed by Delaroche et al./9/ which is ideally suited to find POMP's in the wide energy domain required in nuclear data evaluation. Often, however, experimental data are not available in the full energy and mass range. As POMP's depend on around 12 parameters with pronounced ambiguities between some of them interpolations and in particular extrapolations are difficult. Therefore guidelines provided by the theory of the OMP are very helpful. In the following I will describe some theoretical support referring to nucleon potentials.

The Lane model/10/ defines an OMP which simultaneously applies for protons and neutrons; the nucleon type determines the sign of the the isovector component and the Coulomb correction. Therefore a neutron potential can be derived from a proton potential, in particular if the isovector component is fixed by fitting quasi-elastic (p,n)-scattering. This method was extensively applied and tested by Hansen et al.; for a recent application see Ref./11/. The Lane formalism was also used by Madland/12/ in the development of a global neutron potential for energies ranging from 80 to 180 MeV. As neutron data are scarce in this energy region the starting point was the proton potential by Schwandt et al./13/.

Among the methods to calculate a microscopic optical model potential (MOMP) for nucleons the "nuclear matter approach" seems at present the most suitable one for nuclear data evaluations. The JLM-model, was developed by Jeukene, Lejeune and Mahaux/14-15/. It calculates the nucleon potential in nuclear matter in the framework of the Brueckner-Hartree-Fock approximation starting from Reid's/16/ hard core nucleon-nucleon potential. This nuclear matter potential is conveniently parametrised as function of energy and density. The MOMP for a finite nucleus is obtained by the local density approximation (LDA) or the improved version (ILD) which by means of a range parameter accounts for the finite range of nuclear forces. The energy range of the JLM-potential is from 10 to 160 MeV. Lejeune/15/ proposed an extension below 10 MeV. Other nuclear matter approaches starting from the

Hamada-Johnston/17/ nucleon-nucleon interaction were reported by Brieva and Rook/18/ and more recently by Yamaguchi et al./19/. Also these two models require the nuclear density for the transition from nuclear matter to a finite nucleus. All three models result in a local potential.

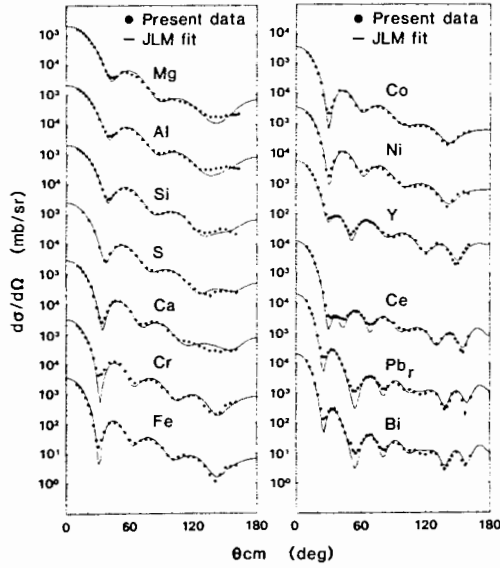


Fig.1 Differential elastic neutron scattering cross sections at $E_n = 21.6$ MeV and fits with the JLM potential (from Ref. 21).

As examples for tests of these MOMP's I mention two recent studies which use homogeneous sets of experimental data covering a broad mass range. Differential elastic neutron scattering cross sections for essentially spherical nuclei were measured at Livermore/20/ and at Studsvik/21/ at incident energies of 14.6 and 21.6 MeV, respectively. The MOMP's were calculated with nuclear densities derived from experimental charge densities. The (real) spin-orbit potential in case of the JLM- and the Brieva-Rook model was derived by folding the nuclear density with an effective interaction given by Bertsch et al./22/. The real and the imaginary central potential were multiplied by normalizing constants λ_v and λ_w which were determined by a least square fit to the experimental data. More details on the calculations of the potentials can be found in Refs.23-24. Reasonable good agreement was achieved with all three potentials in the whole mass range. The best reproduction of both data sets was obtained with the JLM-potential. Fig.1 displays the 21.6 MeV Studsvik data and the JLM fits. Apart from deviations in the minima between $20^\circ - 60^\circ$ for some target nuclei the reproduction compares with that of specific POMP fits. The resulting normalization constants which can be represented by the relations

$$\begin{aligned}\lambda_v &= (0.956 \pm 0.009) - (-1 \pm 1) 10^{-4} A \\ \lambda_w &= (0.921 \pm 0.017) - (4.0 \pm 1.7) 10^{-4} A\end{aligned}$$

are very close to unity and nearly independent of the mass number and thus confirm the applicability of the JLM-approach. Very similar results were obtained for the Livermore data set.

With regard to the "free parameters" λ_v and λ_w these potentials are often called "semi-microscopic" (SMOMP). However, there are essentially only two parameters and one of them (λ_v) is very close to unity. As MOMP's are based on sound theory SMOMP's should yield quite good results in energy and mass regions where experimental data are lacking. Some caution is required at low incident energies, say below 10 MeV, where the underlying approximations for the imaginary part are less reliable and effects of finiteness of the nucleus become more important. In an analysis of neutron scattering from ^{208}Pb and ^{209}Bi for energies between 1.5 and 11 MeV Annand et al./5/ obtained energy independent λ_v -values close to unity. However, the normalizations λ_w were substantially smaller than unity at the low energy end and increased with energy.

SMOMP's were also used for deformed nuclei/11,25/. In this case coupled channels calculations are required. Most investigations used microscopic nuclear densities derived by Hartree-Fock-Bogoliubov calculations. Apart from these new features the results correspond to those for spherical nuclei as far as agreement with

experiment and values of the normalizations are concerned.

Recently Mahaux together with Jaminon and Jeukenne/26/ investigated several features of the real part $V(r,E)$ of POMP's for nucleons found by fitting angular distributions in the mass region $10 < A < 80$. To this end they extracted from the empirical potentials the radial moments

$$[r^q](E) = \frac{4\pi}{A} \int dr V(r,E) r^q, \quad (1)$$

which for $0.4 \leq q \leq 4$ are well defined by the experimental data. The ratios of these moments depend only on the geometry of the potential. By comparing empirical moments and moment ratios with those calculated by means of the JLM-approach various properties - as e.g. the dependence of the depth of the real part on A , the difference of the root mean square radii of proton- and neutron potentials and the dependence of the Woods-Saxon shape parameters r_v and a_v on the mass number - could be explained by the theory. This was achieved by the following improvements of the JLM-approach: (i) To correct for shortcomings of the ILDA the surface tail of the real part $V_{JLM}(r)$ of the JLM-potential is fitted by a Woods-Saxon (WS) potential. The three parameters U_v , R_v and a_v of the WS potential $U_v/(1 + \exp((r - R_v)/a_v))$ are given by $U_v = 2V_{JLM}(R_v)$ and $a_v = (r_{0,1} - r_{0,9})$, where r_x is defined by $V_{JLM}(r_x) = xU_v$. (ii) The nuclear densities of neutrons and protons have different shape. When parametrised as WS distributions the neutron diffuseness b_n increases with the asymmetry parameter $(N-Z)/A$ while the proton diffuseness b_p is constant as reflected by the relation: $b_n = b_p(1 + (N - Z)/A)$. This behaviour is explained by the extended Thomas-Fermi approximation of Brack et al./27/. (iii) As in case of direct comparisons with experimental data V_{JLM} is multiplied by a normalization factor close to unity.

Many accurate measurements have accumulated evidence of a change of the properties of the real potential near the Fermi energy. The energy dependence of the depth, in particular if negative energies are included, deviates from the linear decrease observed at higher energies. The geometry depends on energy much stronger than predicted by the JLM-approach/28/. This "Fermi-surface anomaly" which was recently reviewed by Hodgson/29/ takes place in an energy region that for neutrons is of great technological importance. It may also partly be responsible for the troubles with POMP parametrisations at low energies. Recent investigations of the Fermi-surface anomaly for neutrons were reported by the Argonne group/7/.

The basic explanation of this effect, namely the coupling of the single particle degree of freedom to surface excitations of the core, was proposed by Bertsch and Kuo/30/ and further developed by Mahaux and Ngô/31/. In a series of recent papers Mahaux and Sartor/32/ developed the following dispersion relation approach for the investigation of the Fermi-surface anomaly.

The mean nuclear field $V(r,E)$, i.e. at positive energy E the real part of the OMP and at negative energy the shell model potential, is written as the sum of a Hartree-Fock (HF) type contribution $V_{HF}(r,E)$ and a dispersive correction $\Delta V(r,E)$

$$V(r,E) = V_{HF}(r,E) + \Delta V(r,E). \quad (2)$$

The correction $\Delta V(r,E)$ is caused by coupling to the degrees of freedom of the core and thus strongly depends on energy near the Fermi-surface. The HF term on the other hand is a smooth monotonic function of energy. A dispersion relation allows to calculate the second term of Eq.(2) in terms of the imaginary part $W(r,E)$ of the OMP by the following principal value integral

$$\Delta V(r,E) = \frac{1}{\pi} P \int_{-\infty}^{+\infty} dE' \frac{W(r,E')}{E' - E}. \quad (3)$$

This equation represents a constraint for the OMP. At negative energies $W(r,E)$ is defined by the width of the fragmentation of the single particle states. The imaginary part is assumed to be symmetric around the Fermi energy. Eq.(3) is used to determine the radial moments $[r^q]_{HF}(E)$ of the HF contribution by a fitting procedure from the following "input data": the radial moments $[r^q]_V(E_k)$ and $[r^q]_W(E_k)$ of the real and the imaginary part of POMP's at energy E_k and the binding energies E_{nli} of bound orbits; the moments are defined as in Eq.(1). A linear energy dependence is postulated for $[r^q]_{HF}(E)$. If a WS shape is assumed for $V(r,E)$ and $V_{HF}(r,E)$ one

can determine the WS parameters U_V , a_V and r_V from $[r^q]_V(E)$ and $[r^q]_{HF}(E)$, respectively; actually the moments with $q = 0, 2$ and 4 were used. Fig. 2a, taken from Ref./32d/, shows for the system $^{208}\text{Pb} + n$ in the energy range $-20 \leq E \leq 40$ MeV the derived WS parameters for $V(r,E)$ (full curves) and the empirical values (crosses and squares). The results for the HF contribution are represented by dashed curves. The diffuseness for V and V_{HF} was kept fixed at a typical value $a_V = 0.70$ fm as it turned out to be difficult to determine the energy dependence of this quantity. This figure very clearly illustrates the Fermi-surface anomaly: a strong energy dependence of the radius parameter r_V and marked deviations from the linear decrease of the depth U_V . Evidently these effects are due to the dispersive contribution as the parameters of the HF component smoothly depend on energy. Fig. 2b shows the shape of the real potential V and of its two components V_{HF} and ΔV for three values of the energy E relative to the Fermi energy E_F . Near E_F the dispersive contribution is essentially surface peaked. This shape derives from the dispersion relation and the fact that at low energies the imaginary part of a POMP is surface peaked. Recent investigations of the system $^{208}\text{Pb} + n$ for $-20 \leq E \leq 165$ MeV in the frame of dispersion relations were reported by Johnson et al./33/. The dispersion relation approach well explains the anomalies of the real potential. Note, however, that also the imaginary parts of POMP's which enter into the calculation of $\Delta V(r,E)$ often exhibit a strongly energy dependent geometry. Lawson et al./7b/ showed in their investigation of the system $^{209}\text{Bi} + n$ that the strong energy dependence of the diffuseness of the imaginary part of their POMP is only slightly reduced if the dispersive correction is added to the real part. Therefore, from the applied point of view, there remains the problem how to find the energy dependence of the imaginary part in case that accurate experimental data are lacking.

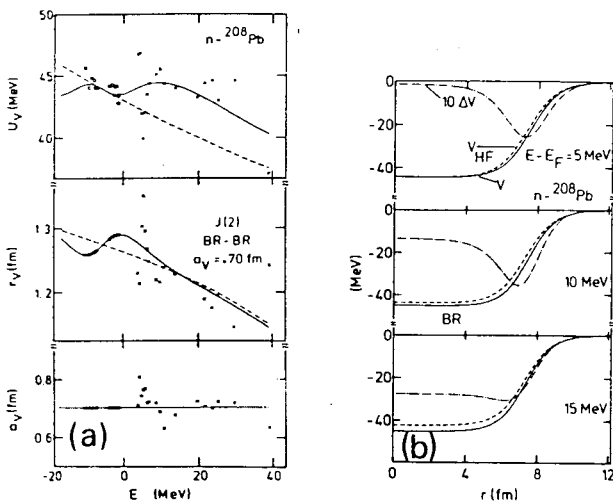


Fig.2 Dispersion relation analysis of the real part $V(r,E)$ of the OMP for $^{208}\text{Pb} + n$. (a) WS parameters. (b) radial dependence of $V(r,E)$ and its two components at three energies (from Ref. 32d)

To conclude this section I refer to a recent semi-microscopic OMP for nucleons which was proposed by a Chinese group/34/. Also this theory is based on the nuclear matter approach and covers non-relativistic and relativistic energies. I emphasized the potentials for nucleons due to their technological importance. Moreover the theory of the OMP for composite particles is more involved than that for nucleons; I refer to a recent review by Leeb/35/.

Compound Nucleus Reactions

The theory of compound nucleus (CN) reactions aims at the calculation of energy averaged cross sections in terms of average S-matrix elements which are obtained from the optical model. So, the desired expressions are generalizations of the celebrated Hauser-Feshbach formula. In spite of much effort for more than two decades it proved very difficult to derive cross section formulas from the statistical properties of resonance parameters. Fit formulae found by Monte Carlo techniques were proposed by Moldauer/36/ and by Hofmann et al./37/; they are used in most computer codes. The effects of direct reactions on CN cross sections can be treated by

means of the Engelbrecht-Weidenmüller transformation/38/.

During the past three years essential progress has been achieved in Hauser-Feshbach theory; an extensive recent review on this topic was presented by Fröhner/39/. The probability distribution of the S-matrix for a given average could be derived by methods of information theory by groups in Mexico/40/ and in Karlsruhe/41/. On the other hand Verbaarschot, Weidenmüller and Zirnbauer/42/ finally succeeded to derive an exact formula under the assumption that the Hamiltonian that generates CN states is an element of the Gaussian orthogonal ensemble (GOE). They represent the average cross section as a threefold integral of an algebraic expression of the transmission coefficients. The properties of the GOE triple integral are further discussed by Verbaarschot/43/ and by Harney and Hüpper/44/.

Of special interest is the comparison of the GOE triple integral with the widely used fit formulas. Verbaarschot/43/ reports good agreement with the Monte Carlo calculations of Hofmann et al./37/ and Fröhner/39/ found for $^{238}\text{U} + n$ agreement with Moldauer's/36/ prescription within 1-3%. So, the result of the formulae which we used so far are not unreasonable. As the GOE triple integral represents a rigorous result it should replace the well known fit formulas; Verbaarschot/43/ reports a reliable code for its evaluation.

Apart from the question of the fundamental cross section formula there are also other problems with CN model calculations. The results critically depend on transmission coefficients for particles and γ -rays and on the levels of the residual nuclei. This, of course, applies also to calculations concerned with multiple particle and γ -ray emission. Some remarks on γ -ray strength functions and on level densities are presented in the following.

The γ -ray transmission coefficients $T_{XL}(E_\gamma)$, where E_γ and XL respectively denote energy and multipole type, are proportional to the γ -ray strength functions $f_{XL}(E_\gamma)$. It has been observed for many years that the E1 strength function is better described by the giant dipole resonance (GDR) model of Brink and Axel/45/ than by the single particle model of Blatt and Weisskopf/46/. This was also recently confirmed by Krusche and Lieb/47/ in the mass region $A = 46-80$. The analysis of many accurate experimental data showed that the GDR model has to be refined in several respects. E1 strength functions obtained by extrapolating one or two Lorentzians based on photoabsorption data overestimate those derived from capture data (see e.g. Refs.48,49). A simple empirical correction is to use a "depressed" giant dipole resonance /50/. Recently Kopecky and Chrien/51/ investigated an approach which is supported by theory. The employed expression assumes a Lorentzian with an energy dependent width $\Gamma(E_\gamma)$ and accounts for a finite limit of $f_{E1}(E_\gamma)$ at $E_\gamma \rightarrow 0$ as proposed by Kadenskij et al./52/

$$f_{E1}(E_\gamma, T) = 8.68 \times 10^{-8} \sigma_0 \Gamma_0 \times \left[\frac{E_\gamma \Gamma(E_\gamma)}{(E_\gamma^2 - E_0^2)^2 + E_\gamma^2 \Gamma(E_\gamma)^2} + \frac{0.7 \Gamma_0 4\pi^2 T^2}{E_0^5} \right] \quad (4)$$

where $\Gamma(E_\gamma) = \Gamma_0(E_\gamma^2 + 4\pi^2 T^2)/E_0^2$ and $\Gamma_0 = \Gamma(E_0)$. The quantities σ_0 and E_0 represent the peak cross section and the resonance energy; T is the temperature corresponding to the excitation energy. Fig. 3, taken from Ref.51, shows for ^{106}Pd the E1 strength function parametrised according to Eq.(4) and experimental data. Note that the dependence on the temperature represents a departure from Brink's hypothesis /45a/ that the form of the photoabsorption cross section is the same for ground and for excited states. A general theoretical investigation on dipole strength functions was recently published by Sirotkin/53/. For heavy nuclei a bump observed in γ -ray production spectra is often explained by a E1 pygmy resonance. A recent study of the systematics of this resonance for nuclei with $N \approx 82 - 126$ was reported by Igashira et al./54/.

There is growing evidence that also the M1 strength function can be related to a giant resonance with a peak between 8-9 MeV and a width of several MeV/55/; a pertinent model, based on spinflip excitations was proposed by Bohr and Mottelson/56/. By means of average resonance capture of 2 and 24 keV neutrons in ^{105}Pd Kopecky and Chrien/51/ studied the energy dependence of the M1 strength. It is consistent with a giant resonance around 8.8 MeV and a width of about 4 MeV. For cross section calculations E1 and M1 strength functions are the most important ones. Surveys on quadrupole strength functions are reported in Refs.57,58.

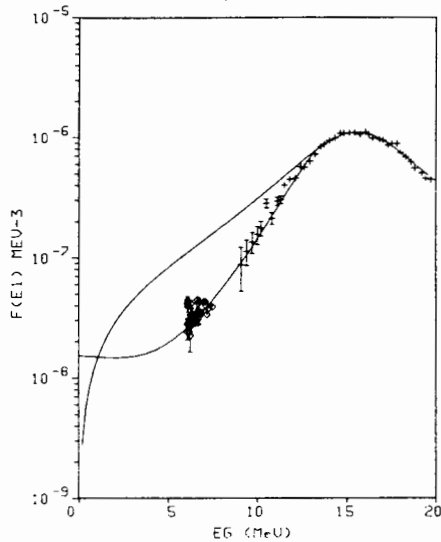


Fig.3 The E1 strength function for ^{106}Pd . The crosses are derived from (γ, n) - and the open squares from (n, γ) data, respectively. The lower curve corresponds to Eq.(4) and the upper curve to the conventional GDR parametrization (from Ref. 51).

Several recent papers illustrate that with suitably chosen γ -ray strength functions a satisfactory reproduction of capture cross sections and of γ -ray production spectra can be achieved for incident energies up to a few MeV. I mention the capture cross sections for $^{150,153}\text{Eu}$ and $^{185,187}\text{Re}$ which were investigated by Macklin and Young/59/. For Eu the energy dependence of the E1 strength functions was taken from data of nearby nuclei (spectrum fitting for ^{170}Tm) and for Re photonuclear data were used. The γ -strength functions were normalized to reproduce the ratio $\langle \Gamma_{\gamma 0} \rangle / \langle D_0 \rangle$ of the average total radiation width and the average resonance spacings for s-waves. Successful capture calculations for ^{197}Au were reported by Joly/60/ and for ^{181}Ta and ^{197}Au by Yamamuro et al./61/. Naturally the good reproduction of capture data by CN model calculations is restricted to lower incident energies where this mechanism dominates. For higher incident energies direct and semidirect capture must be accounted for.

Most CN model applications require information on level densities. In the past years microscopic methods to calculate this quantity have been developed. Microscopic Fermi gas calculations, as e.g. described by Moretto and Huizenga/62/, start from given single particle levels and a simple pairing force as residual interaction. The resulting level density, which is deduced by the BCS formalism and by statistical methods (partition function, saddle point approximation), refers to intrinsic states. Simple enhancement factors accounting for collective excitations were discussed by Björnholm et. al/63/. The problems which arise when applying collective enhancement factors to the results of microscopic Fermi gas calculations, in particular in an extended energy range, were surveyed by Grimes/64/. Another microscopic method, the spectral distribution approach, was developed by French and co-workers/65/ and refined later on by many authors; for a recent application see e.g. Ref.66. As this approach accounts for full two-body residual interactions it is not affected by the problems of collective enhancement.

In spite of the availability of these microscopic methods most applied cross section calculations employ phenomenological approaches which start from the Fermi gas formula for the density $\rho(U, I)$ of levels around excitation energy U with spin I

$$\rho(U, I) = \frac{2I+1}{24\sqrt{2}\sigma^3 a^{1/4} U^{5/4}} \exp\left\{2\sqrt{a}U - \frac{(I+1/2)^2}{2\sigma^2}\right\}, \quad (5)$$

where $\sigma = \sigma(U)$ denotes the spin cut-off factor. This formula is derived for non-interacting nucleons and equidistant levels. Popular are the Gilbert-Cameron model (GCM) /67/ which combines a constant temperature form $\rho(U, I) \propto \exp[U/T - (I+1/2)^2/2\sigma^2]$, used at low energies, with Eq. (5), and the back-shifted Fermi gas model (BSFGM) /68/. While in the GCM Eq. (5) is corrected for

pairing by the replacement $U \rightarrow U - \Delta_p$, where Δ_p is obtained from the respective mass differences, the BSFGM employs a back-shift Δ_b which is considered a free parameter. The parameters of these models - essentially (a, T) and (a, Δ_b) for GCM and BSFGM, respectively - are found by fitting the densities of low lying levels and of resonances and hence are based on data in a narrow energy range. They reflect the properties of the single particle states around the Fermi energy; as a consequence the parameter a in Eq. (7) exhibits pronounced shell effects. Microscopic calculations show that these shell effects are washed out with increasing excitation energy. Therefore these phenomenological models should be used only in regions where they are supported by experimental data. Recently von Egidy et al./69/ showed that both, the constant temperature form and the BFGM, represent experimental level densities up to the neutron binding energy equally well. This work was based on extensive and complete level schemes and resonance spacings in the mass region $A = 20-244$. Thus, the use of these approaches for relatively low incident energies as in the previously mentioned capture calculations /59-61/ is justified. However, the extrapolation of the results to higher energies and/or nearby nuclei is difficult.

To overcome these drawbacks improved level density formulae were proposed which are still simple enough to be attractive for routine calculations. I mention two methods which relate the shell effects of the level density to the ground state shell correction $\delta W = M_{\text{exp}} - M_{\text{drop}}$ defined as difference of the experimental and the liquid drop mass/70/. The first one was developed by Ignatyuk and co-workers/71/ and essentially employs in Eq. (7) an excitation energy dependent parameter: $a(U) = \bar{a}(1 + \exp(-\gamma U)\delta W/U)$, where \bar{a} is the asymptotic value. This approach was further refined by applying simple collective enhancement factors and by accounting for pairing correlations/72/. A recent application to the calculation of fission cross sections is reported in Ref.73. The second method was proposed by Kataria et al./74/. It starts from a Fourier expansion of the shell fluctuations of the single particle state density and is, as pointed out by the authors/75/, closely related to the model of Ignatyuk et al./71/. As an application of the approach of Ignatyuk et al./71/ asymptotic level density parameters \bar{a} were deduced from recent data on s-wave resonances for protons/76/ and neutrons/77/ in the mass range $A = 40-66$. Fig.4a shows that in this relatively narrow mass range \bar{a} is well described by a linear function of the mass number $\bar{a} = 0.133A$; the minimum χ^2 was obtained with $\gamma = 0.093$. These values can be used in this mass region for nuclei with no resonance data. Fig.4b displays the analogous ratio a/A for the Fermi gas formula Eq.(5) resulting from the same experimental data. Different shell corrections are responsible for the more complicated dependence on the mass number. The asymptotic parameters shown in Fig.4a were deduced under the following assumptions: no vibrational enhancement, pairing correction according to Ref./67/, rigid body moment of inertia for the calculation of the spin cut-off factor and parity independence of the level density near the nucleon separation energy. Therefore these parameters are affected by additional uncertainties. Nevertheless, the smooth behaviour as a function of the mass number should persist.

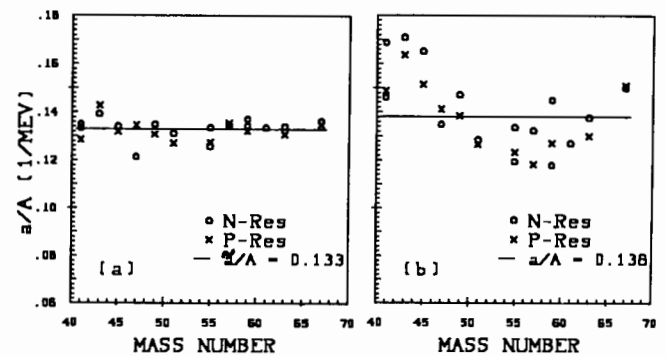


Fig.4 Level density parameters deduced from average resonance spacings: (a) asymptotic a -parameter of the model of Ignatyuk et al./71/. (b) a -parameter in Fermi-gas formula Eq.(5).

The parity dependence of the level density was recently discussed by Mengoni et al./78/ on basis of a microscopic Fermi gas model/79/; a phenomenological description of parity effects was

proposed, too. The parity dependence is of special importance if the average spacing of s-wave resonances is used to deduce total level densities. Accurate measurements indicate for lighter nuclei a significant difference in the density of states of different parity (see e.g. Ref.80). Jacquemin and Kataria/81/ developed an efficient and exact recursive method to calculate the level densities as function of energy, spin and parity for non-interacting fermions. Their results for Ca isotopes show differences in the densities of states of opposite parities for energies up to 40-60 MeV. Recently Grimes/82/ pointed out that the microscopic Fermi gas approach to calculate the parity dependence from the average occupation probability fails. This was shown for non-interacting fermions by comparison with the exact results according to Jacquemin and Kataria/81/.

Direct Reactions

At higher incident energies the population of low lying levels by binary processes is often dominated by direct reaction (DI) contributions. Their treatment requires specific models depending on the structure of the levels.

Because of the relatively large cross sections DI inelastic scattering is of great applied interest. Due to their simplicity the preferred models are those which are based on POMP's and on macroscopic collective models as the harmonic vibrational model or the axial rotor model. The calculations are performed by means of computer codes employing either the Distorted Wave Born Approximation (DWBA) or the coupled channels (CC) formalism.

As an example for the application of such macroscopic models I refer to the extensive analyses of inelastic neutron scattering from the principle even actinides performed by Sheldon et al./83/. The incident energies range from threshold to about 3 MeV and thus CN- and DI contributions must be considered. The latter, calculated by the CC method, comprise the excitation of rotational bands built on the ground state and on quadrupole and octupole vibrational states. Due to limitations in memory and computation time only a restricted number of levels can be coupled in one run. Recent results of this work are described in this conference. So I will mention only one special feature of these calculations. For the level excitation functions the effects of direct reactions on the CN-contributions are considered in the framework of the approach by Hofmann et al./37/ which uses the Engelbrecht-Weidenmüller transformation/38/. In an analysis of inelastic neutron scattering from ^{238}U Shao et al./84/ used the DWBA for the excitation of states of the higher vibrational bands. The CC calculation was restricted to the ground state rotational band and so computation time could be saved. The deformation parameters for the DWBA were taken from charged particle Coulomb excitation and inelastic scattering data. Similar calculations for ^{235}U are presented by Arthur and Young in this conference.

Many evaluations use macroscopic models to assess DI contributions to (n,n')-reactions on spherical nuclei. Here I mention an application by Ignatyuk et al./85/ which is related to the physical reasons for the dispersive contribution to the real part of the OMP. The object was the calculation of the s-, p- and d-wave neutron strength functions for the structural materials around iron, which are notorious for difficulties with POMP parametrisations. This approach is called "multi-channel coupling method" as it considers the coupling of around 20 one- and two-phonon states with real form factors. A good reproduction of experimental data was obtained with a POMP with the same geometry for all considered nuclei. The absorptive component is small as the coupling to the most important degrees of freedom is explicitly accounted for.

The application of these macroscopic models requires the knowledge of deformation parameters. For incident neutrons this information is not always available. In this case parameters are often deduced from charged particle inelastic scattering and from electromagnetic transitions. This is convenient but not necessarily correct. Madsen et. al./86/ discuss in the framework of a schematic model/87/ differences of the quadrupole deformation parameters obtained with different probes for vibrational nuclei. These differences show up for single closed shell nuclei and diminish for open shell nuclei. Deformation parameters of permanently deformed nuclei deduced from neutron and proton scattering show no systematic differences (see Refs. 88,89).

As pointed out by Delaroche/90/ simple collective models as the harmonic vibrator- or the rigid rotor model are not appropriate

for soft nuclei in transition regions. More sophisticated nuclear structure models as the "dynamic deformation model"/91/ or the "interacting boson approximation"/92/ are required; as a recent example I refer to an investigation of inelastic neutron scattering from ^{194}Pt by Hicks et al./8/. Kumar et al./93/ proposed an extended CC method for baryon scattering based on the Bohr Hamiltonian with microscopically calculated potential energy and inertial parameters. Semi-microscopic calculations of inelastic nucleon scattering, which are based on the JLM microscopic optical potential, were reported by Lagrange and Brient/94/ for ^{208}Pb and by Lagrange et al./25,95/ for heavy deformed nuclei. These calculations start from microscopic nuclear densities derived by the Hartree-Fock-Bogoliubov method. To generate the coupling potentials for deformed nuclei these densities are expanded in a Legendre polynomial series. In case of the vibrator ^{208}Pb the transition densities were derived from the random phase approximation and folded with the effective JLM-interaction. As a recent example of microscopic DWBA calculations with various models for the transition density I refer to a paper by Mellema et al./96/. A general formalism for the CC description of inelastic scattering in the framework of microscopic collective models was developed by Delaroche and Dietrich/97/.

In connection with inelastic scattering calculations I refer to a new version of one of the most effective CC programs, namely Raynals ECIS code/98/. The new version includes a relativistic treatment of elastic and inelastic scattering employing the Dirac formalism. Furthermore it allows the treatment of CN reactions in presence of DI as proposed by Moldauer/99/. The new code is now available from the NEA Data Bank.

Other DI contributions of applied interest are those from capture and from transfer reactions. I will restrict myself to a few remarks on the latter. Interesting DI analyses of (p, α)- and (n, α)-reactions were performed by Gadioli et al./100/ in the framework of a semi-microscopic model developed by Smits et al./101/. This model employs the DWBA with bound cluster form factors. The spectroscopic amplitudes are related to the spectroscopic factors of one- and two-nucleon transfer reactions. An overall normalization factor, which is the same for all levels and does not depend on the incident energy, is required for the reproduction of the absolute cross section. Calculations based on the pickup mechanism reasonably well reproduced experimental cross sections for $^{90,91}\text{Zr}(n, \alpha)$ with the same normalization factor for both target nuclei. A slightly less satisfactory reproduction resulted from the knockout mechanism. Recently coherent pickup and knockout contributions were considered for the reaction $^{146}\text{Nd}(p, \alpha)/100c/$.

As an example for another type of direct reactions I mention a paper by Mustafa et al./102/. It concerns activation cross sections and isomeric ratios for the (p,n)- and (d,2n) reaction on ^{52}Cr . A conventional calculation based on the CN model and the exciton model reproduced the experimental data for the (p,n) reaction but failed in case of the (d,2n) reaction. The calculated activation cross sections were too large and the isomeric ratios too small. A decisive improvement was achieved by (i) reducing the optical model absorption cross section in order to correct for direct reactions (mainly deuteron breakup) which don't lead to fusion and (ii) by including processes where the breakup is followed by the absorption of the proton ("breakup fusion").

Preequilibrium decay

With the growing demand for reaction data at higher incident energies models for preequilibrium (PE) decay become more and more important. The past years have witnessed many applications of two theoretical approaches which rely on a quantum mechanical treatment: the model of Feshbach, Kerman and Koonin/103/ and that of Tamura, Udagawa and Lenske/104/. Recent reviews on results obtained with these models were presented by Bonetti/105/ and Marcinkowski/106/. I will mainly concentrate on phenomenological models which are used for routine calculations. The two most popular of these models are the Exciton model (EM) and the Hybrid model (HM) which were recently reviewed by Gruppelaar and Akkermans/107/ and by Blann/108/, respectively.

The long debated conceptual differences between EM and HM (see Ref.109) were re-investigated by Akkermans/110/ and by Bisplinghoff/111/. The EM assumes states with maximum config-

uration mixing and calculates exclusive spectra. The HM, on the other hand, relies on essentially independent excitons and yields inclusive spectra. This causes difficulties when the HM (combined with the CN model) is applied to calculate production cross sections for the residual nuclei. In a recent review Blann/112/ illustrated that simple corrections for multiple PE emission (Ref.113) quite successfully reproduce a variety of experimental data as nucleon induced reactions with incident energies up to 200 MeV or reactions following the capture of stopped negative pions. A more rigorous and complicated treatment of multiple PE emission is provided by the exclusive version of the INDEX model (independently interacting excitons) which was proposed by Ernst et al./114/ as an extension of the HM. The consideration of multiple PE emission is no problem for the EM due to its exclusive character/115/. EM based calculations which consider multiple PE processes were reported by Arthur et al./116/. Bisplinghoff/111/ pointed out that the exciton distribution functions in terms of Ericson type state densities should be improved for both models. It was shown, however, in Ref./117/ that in case of the HM these improvements have little impact on angle integrated spectra.

An important extension of the EM represents the inclusion of angular momentum and parity conservation which was recently described in papers by Shi Xiangjun et al./118/, Obložinský/119/, Ryckbosch et al./120/ and Fu/121/; these also contain references to earlier work. This development is important for two reasons. (i) In the frame of the master equation approach/118/ it leads to a "unified model" with the Hauser-Feshbach formula as equilibrium limit. (ii) It makes possible to calculate the PE contribution to discrete level populations and to isomeric state production cross sections. Shi Xiangjun et al./118/ proposed quite accurate approximations which speed up the spin-parity dependent calculations so that they are fast enough for applications. These approximations mainly rely on the weak angular momentum dependence of the transition- and emission rates which seems also to be the reason for the very small impact of angular momentum on the calculated emission spectra. So, for many applications one can safely use the spin and parity independent EM. HM calculations with angular momentum and parity taken into account were recently reported by Avrigeanu et al./122/.

Many EM formulations consider only one type of nucleons and successfully correct for neutron proton distinguishability. Papers dealing with a two-component model (Refs.123-125) were recently reviewed by Kalbach/126/. The results of the extended model depend on the transition rates corresponding to the interaction of (p,p)-, (n,n)- and (p,n)-pairs. Kalbach showed that both, the one- and two-component model, yield practically the same particle spectra if similar assumptions regarding the strength of the different interactions are made. Though more complicated the two-component model offers the advantage that phenomena which critically depend on neutrons and protons like pairing or shell effects can be treated in a more realistic way. A two-component exciton model is presented in this conference by Herman et al.

An essential extension of PE models represents the development of proper emission rates for gamma-rays. I refer to two recent papers which contain also references to previous work. Akkermans and Gruppelaar/127/ proposed an approach in the framework of the spin-parity independent EM. They consider only E1-transitions and derive emission rates which are consistent with the equilibrium limit from the Brink-Axel model/45/. The generalization to the case of angular momentum coupling was reported by Obložinský/119/. Similar as in the case of particle emission the impact of angular momentum is small. Preequilibrium gamma-ray emission provides a simple way to assess direct and semidirect capture processes and thus to describe the high energy tail of the gamma-ray production spectra at higher incident energies. For energies far beyond the maximum of the giant dipole resonance two particle radiative processes become important. Remington et al./128/ propose as source of high energy γ -rays in heavy ion reactions the bremsstrahlung emitted in incoherent neutron proton collisions. A recent extensive review on PE emission of γ -rays which also includes some HM applications was presented by Obložinský/129/.

The treatment of PE emission is more involved for complex particles (d,t, ^3He , α) than for nucleons. The HM does not consider complex particle emission at all. The EM underpredicts experimental data by far if standard emission rates based on detailed bal-

ance are used/130/. Therefore many extensions of the EM for complex ejectiles have been devised. Kalbach/130/ developed simple phenomenological expressions for direct reaction contributions to be added to the EM results. A general method was developed by Iwamoto et al./131/ who assume that a cluster with x nucleons is formed from m particles above and $l=m-x$ particles below the Fermi energy. So, in contrast to the standard EM assumptions, clusters may be emitted from configurations with particle numbers $p < x$. In fact, cluster formation factors assessed in the frame of the Fermi gas model show that for lower incident energies the clusters with a maximum number of particles below the Fermi energy are favoured. Therefore in this model the pickup mechanism dominates cluster emission. Comparisons to experimental angle integrated spectra resulting from p-induced reactions at $E_p = 62$ MeV/132/ showed good agreement for alphas and a fair reproduction of the general features for d, t and ^3He . At the high energy end the experimental spectrum is underpredicted, especially for deuterons. Many models for the emission of α -particles are based on the assumption of knockout of preformed clusters (Refs.133-135). Some of them were recently reviewed by Gadioli/136/.

All models for complex particle emission mentioned so far do not consider angular momentum conservation. Bisplinghoff and Keuser/137/ pointed out that angular momentum effects are very important for cluster emission - in particular for composite systems formed in states with large spin. In the framework of the EM with angular momentum conservation but with detailed balance based emission rates they reproduced the ratios of α - to proton emission cross sections for α - and heavy ion induced reactions. It turned out that for the ^{66}Zn composite system angular momentum conservation causes α -emission to dominate nucleon emission for angular momenta exceeding 15 units.

The density of states with fixed numbers of excited particles and holes (p-h state densities) plays a crucial role in PE models. A comprehensive study of this problem for an arbitrary single particle Hamiltonian was reported by Blin et al./138/. Fu/139/ found simple numerical solutions of the pairing equations for a one-component system as formulated by Ignatyuk et al./140/. In this way BCS calculations of the p-h state densities and of the corresponding spin cutoff factors became feasible for routine calculations. Fu's solutions were also used by Kalbach/141/ for a slightly improved p-h state density formula. A general combinatorial approach to calculate for p-h configurations the state density and the spin- and parity distributions under consideration of the pairing interaction was developed by Herman and Reffo/142/. These calculations start from realistic single particle levels and apply to a two-component system. Thus the results can be used in realistic PE calculations to study e.g. effects of shell structure; the computational effort of this approach is large.

Shell effects in PE emission spectra are related to the p-h state densities. A recent example of neutron spectra resulting from proton bombardment of lead isotopes was reported by Harder et al./143/. The high energy tail of the neutron spectra could be reproduced only by a microscopic state density resulting from realistic single particle states and not by simple expressions based on equidistant levels. Kumabe et al./144/ investigated shell effects in terms of the "modified uniform spacing model" for the p-h state densities; results are presented also in this conference.

As phenomenological PE models do not account for direct reactions populating levels with specific structure one has to add appropriate DI contributions. This holds in particular for inelastic scattering and collective levels. As an illustration Fig.5a shows a recent evaluation (Ref.145) of the neutron production spectrum for $\text{Ni} + n$ at $E_n = 14.1$ MeV and the results of model calculations performed with the code MAURINA/146/. The dashed curve was obtained under consideration of the CN model with multiple particle emission and the EM while for the full curve also direct DWBA contributions to levels with known deformation parameters β_λ are included. On the other hand, as displayed in Fig.5b, the same calculations without direct (n,p) contributions reasonably well reproduce the proton production spectrum for $^{58}\text{Ni} + n$ measured by Grimes et al./147/. The importance of direct processes for the hard

component of (n,n') spectra was recently stressed by Ignatyuk et al./148/. By considering a large number of collective one and two phonon states (n,n') spectra for incident energies of 14.5 and 25.7 MeV could be well reproduced. A problem arises for nuclei with incomplete information on dynamic deformation parameters β_λ at higher excitation energies. This occurs often for vibrations of higher multipolarity $\lambda > 3$. In such cases Ignatyuk et al./148/ suggest to resort to theory, i.e. to use microscopic calculations for the strength $\beta_\lambda^2(U)$ of coherent excitations of multipole type λ fitted to reproduce the data of the lowest collective states.

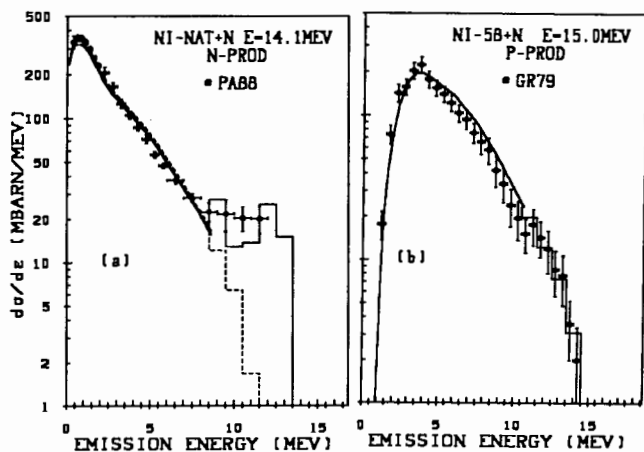


Fig.5 Angle integrated spectra (open symbols) for (a) $^{68}\text{Ni}(n,xn)$ and (b) $^{68}\text{Ni}(n,xp)$ at $E_n = 14.1$ and 15.0 MeV, respectively compared to model calculations (curves and histograms); see text.

In the context of inelastic nucleon scattering I refer also to an interesting model developed by Kalka et al./149/. This model with remarkably simple final formulas starts from the concept of Feshbach et al./103/. The multistep direct contribution accounts for two steps involving excitons and/or phonons; the multistep compound contributions start with an initial exciton number of 5.

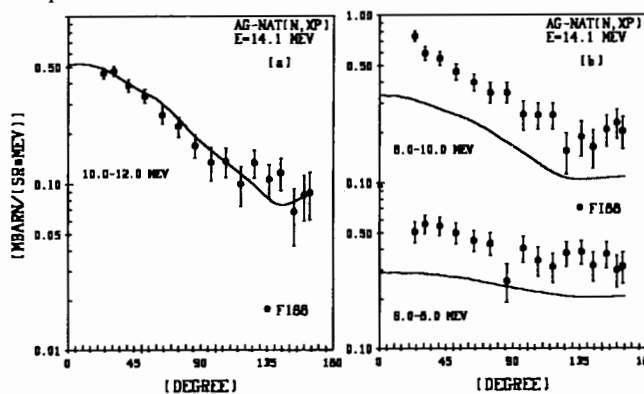


Fig.6 Angular distributions (open symbols) for $^{107}\text{Ag}(n,px)$ at $E_n = 14.1$ MeV compared to model calculations (curves); see text.

The calculation of angular distributions in the EM or the HM is mostly based on the concept of the fast particle/150/. Recent developments (Refs.151-153) account for angle-energy correlations by using the scattering kernel given by Kikuchi and Kawai/154/. Some authors correct for refraction in entrance and exit channel. A common feature of these calculations which were recently reviewed by Machner/155/ is an underprediction of the cross sections at backward angles. This is probably due to their classical concepts. However, also models based on quantum mechanics may encounter difficulties. As an example Fig.6 shows the (n,p) double differential cross section for Ag at $E_n = 14.1$ MeV/156/ compared to the predictions of the one-step version of the model of Tamura et al./104/; the calculations consider a (small) Hauser-Feshbach contribution, too. The parameters which essentially determine the magnitude of the cross sections -in this case effective deformations β_λ - were adjusted to reproduce the data for the proton group with the highest energy (Fig.6a). The shape of the angular distributions is reasonably

reproduced in all cases while the absolute cross sections are definitely too small for the lower proton energy groups (Fig.6b). Similar results were also obtained for $^{93}\text{Nb}(n,p)$ /157/.

An interesting approach to angular distributions in the framework of the EM was proposed by Fu/121/. Forward peaked angular distributions are obtained by assuming in the earliest stage of the equilibration process correlations between S-matrix elements of different total angular momentum. Good reproductions of experimental data at incident energies of 14 and 27.5 MeV were obtained with an energy independent correlation coefficient of 0.5.

Especially valuable for routine calculations of angular distributions are the Kalbach-Mann systematics/158/. Recently Kalbach/159/ developed new systematics which apply for incident energies up to 600 MeV. Applications of these systematics are described by Arthur et al./116/ and by Bozoian/160/.

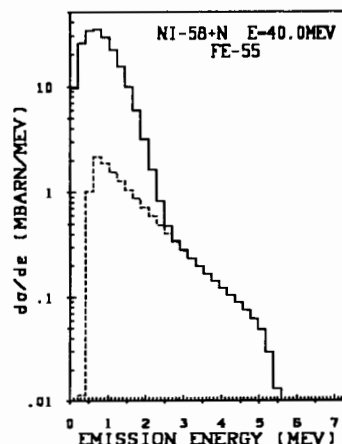


Fig.7 Angle integrated recoil spectrum for ^{55}Fe resulting from $^{68}\text{Ni} + n$ at $E_n = 40$ MeV; see text.

As an application of the models described so far I mention the calculation of the kinetic energy distribution of the heavy reaction products. These "recoil spectra" are important for the assessment of radiation damage and for medical radiation therapy. An iterative procedure to calculate these spectra for reactions with multiple particle emission was recently developed/161/ and incorporated into the code MAURINA/146/. By means of the kinematics of binary reactions the recoil energy distribution for each first chance product is calculated as function of the excitation energy. Higher chance emission is treated as decay in flight. While for first chance processes angular distributions are accounted for eventual directional correlations between successively emitted particles are neglected. As an example Fig.7 shows the LAB-system angle integrated recoil spectrum of ^{55}Fe resulting from the reaction $^{68}\text{Ni} + n$ at $E_n = 40$ MeV with γ , n,p and α as considered emitted particles. Under these conditions ^{55}Fe is produced by first chance alphas or by emission of two neutrons and two protons in 6 different orders. The dashed curve in Fig.7 represents the contributions of the alphas which due to forward peaked PE contributions increases with decreasing energy. The full curve represents the total recoil spectrum; the low energy maximum reflects the contributions of the four nucleons.

Conclusion

Even the small selection of models discussed in this presentation allows the calculation of many cross sections of interest. An important problem is the accuracy of the results -in particular in cases where no experimental data are available. There are two sources of uncertainties. The first one reflects incomplete knowledge of model parameters as e.g. those of POMP's or of level density formulae. Obviously, the effects on the calculated cross sections can be found by sensitivity studies -see e.g. Ref.162. A proposal, how to store in ENDF format the covariances of the parameters and the resulting sensitivities has been worked out by Muir/163/. The second and more troublesome source of uncertainties is due to deficiencies of the models themselves. Their contribution can be assessed only by comparison with experimental data. Uncertainties of this type represent a challenge to improve the models and to extend the experimental data base. Many of the contributions to this conference are good examples for these efforts.

REFERENCES

1. P.E. Young: Proc. Specialists' Meeting on the Use of the Optical Model for the Calculation of Neutron Cross sections below 20 MeV (OECD, Paris, 1986), p.127
2. J. Rapaport, V. Kulkarni and R.W. Finlay: Nucl. Phys. A330, 15(1979)
3. R.L. Walter and P.G. Guss: in Proc. Int. Conf. Nucl. Data for Basic and Applied Science, Santa Fe, N.M., U.S.A., May 13-17 1985, edited by P.G. Young et al. (Gordon and Breach, New York, 1986), Vol. 2, p.1079
4. A.B. Smith, R.D. Lawson and P.T. Guenther: Ref. 1, p.183
5. J.R.M. Annand, R.W. Finlay and F.S. Dietrich: Nucl. Phys. A443, 249(1985)
6. G.M. Honoré et al. Phys. Rev. C33, 1129(1986)
7. R.D. Lawson, P.T. Guenther and A.B. Smith: Phys. Rev. C34, 1599(1986); (b) Phys. Rev. C36, 1298(1987)
8. S.E. Hicks et al.: Phys. Rev. C36, 73(1987)
9. J.P. Delaroche, Ch. Lagrange and J. Salvy: IAEA-190, Vol.1 (Vienna, 1976), p.251
10. A.M. Lane: Phys. Rev. Lett. 8, 172(1962); (b) Nucl. Phys. 35, 676(1962); (c) Nucl. Phys. 37, 663(1962)
11. L.F. Hansen et al.: Phys. Rev. C34, 2075(1986)
12. D.G. Madland: Proc. of IAEA Advisory Group Meeting on Nuclear Theory for Fast Neutron Data Evaluation, Beijing, 12-16 Oct. 1987, to be published; (b) Ref. 35
13. P. Schwandt et al.: Phys. Rev. C26, 55(1982)
14. J.-P. Jeukenne, A. Lejeunne and C. Mahaux: Phys. Rev. C15, 10(1977); (b): Phys. Rev. C16, 80(1977)
15. A. Lejeunne: Phys. Rev. C21, 1107(1980)
16. R.V. Reid: Ann. Phys. (N.Y.) 50, 411(1968)
17. T. Hamada and I.D. Johnston: Nucl. Phys. 34, 382(1962)
18. F.A. Brieva and J.R. Rook: Nucl. Phys. A291 299(1977); (b): Nucl. Phys. A291 317(1977)
19. N. Yamaguchi, S. Nagata and T. Matsuda: Progr. Theor. Phys. 70, 459(1983)
20. L.F. Hansen et al.: Phys. Rev. C31, 111(1985)
21. N. Olsson et al.: Nucl. Phys. A472, 237(1987)
22. G. Bertsch, J. Borysowicz, H. McManus and W.G. Love: Nucl. Phys. A284, 399(1977)
23. S.M. Mellema, R.W. Finlay, F.S. Dietrich and F. Petrovich: Phys. Rev. C28, 2267(1983)
24. F.S. Dietrich et al.: Phys. Rev. Lett. 51, 1629(1983)
25. Ch. Lagrange, D.G. Madland and M. Girod: Phys. Rev. C33, 1616(1986)
26. M. Jaminon, J.-P. Jeukenne and C. Mahaux: Phys. Rev. C34, 468(1986); (b) M. Jaminon and C. Mahaux: Phys. Rev. C34, 2084 and 2097(1986)
27. M. Brack, C. Guet and H.-B. Høkansson: Phys. Rep. 123, 275(1985)
28. C. Mahaux and R. Sartor: Phys. Rev. C34, 2119(1986)
29. P.E. Hodgson: Ref. 12a
30. G.F. Bertsch and T.T.S. Kuo: Nucl. Phys. A112, 204(1968)
31. C. Mahaux and H. Ngô: Nucl. Phys. A379, 205(1982)
32. C. Mahaux and R. Sartor: Nucl. Phys. A458, 25(1986); (b) Nucl. Phys. A460, 466(1986); (c) Phys. Rev. C36, 1777(1987); (d) Nucl. Phys. A468, 193(1987); (e) Nucl. Phys. A475, 247(1987)
33. C.H. Johnson, D.J. Horen and C. Mahaux: Phys. Rev. C36, 2252(1987)
34. Gu Yingqi et al.: Ref. 12a
35. H. Leeb: Proc. Specialists' Meeting on Preequilibrium Nuclear Reactions, NEANDC of OECD, Semmering, Austria, 10-12 Febr. 1988, to be published.
36. P.A. Moldauer: Nucl. Phys. A344, 185(1980)
37. H.M. Hofmann, J. Richert, J.W. Tepel and H.A. Weidenmüller: Ann. Phys. (N.Y.) 90, 403(1975)
38. C.A. Engelbrecht and H.A. Weidenmüller: Phys. Rev. C8, 859(1973)
39. F.H. Fröhner: Ref. 12a
40. P.A. Mello, P. Peyreya and T.H. Seligman: Ann. Phys. (N.Y.) 161, 254(1985)
41. F.H. Fröhner: Rad. Effects 96, 199(1986)
42. J.J.M. Verbaarschot, H.A. Weidenmüller and M.R. Zirnbauer: Phys. Rep. 129, 367(1985)
43. J.J.M. Verbaarschot: Ann. Phys. 168, 368(1986)
44. H.L. Harney and A. Hüpper: Z. Phys. 328, 327(1987)
45. D.M. Brink: Oxford Univ. thesis (1955), unpublished (b) P. Axel: Phys. Rev. 126, 671(1962)
46. J.M. Blatt and V.F. Weisskopf: Theoretical Nuclear Physics (Wiley, New York, 1952)
47. B. Krusche and H.P. Lieb: Phys. Rev. C34, 2103(1986)
48. C.M. McCullagh, M.L. Stelts and R.E. Chrien: Phys. Rev. C23, 1394(1981)
49. K. Nilson et al.: Nucl. Phys. A475, 207(1987)
50. S. Joly, D.M. Drake and L. Nilsson: Phys. Rev. C20, 2072(1979)
51. J. Kopecky and R.E. Chrien: Nucl. Phys. A468, 285(1987)
52. S.G. Kadenskij, V.P. Markushev and V.I. Furman: Sov. J. Nucl. Phys. 37, 165(1983)
53. V.K. Sirotkin: Sov. J. Nucl. Phys. 43, 362(1986)
54. M. Igashira et al.: Nucl. Phys. A457, 301(1986)
55. J. Kopecky: Ref. 3, Vol. I, p. 967
56. A.G. Bohr and B.R. Mottelson: Nuclear Structure, (Benjamin, London 1975) Vol. II, p. 636
57. J. Kopecky: Capture Gamma-ray Spectroscopy and Related Topics, 1984 (American Institute of Physics, New York, 1985) p. 318
58. W.V. Prestwich, M.A. Islam and T.J. Kennet: Z. Phys. A315, 103(1984)
59. R.L. Macklin and P.G. Young: Nucl. Sc. Eng. 95, 189(1987); (b) Nucl. Sc. Eng. 97, 239(1987)
60. S. Joly: Nucl. Sc. Eng. 94, 94(1986)
61. N. Yamamuro, K. Udagawa and T. Natsume: Nucl. Sc. Eng. 96, 210(1987)
62. J.R. Huizenga and L.G. Moretto: Annu. Rev. Nucl. Sci. 22, 427(1972)
63. S. Bjørnholm, A. Bohr and B. Mottelson: Proc. of the third IAEA Symposium on The Physics and Chemistry of Fission, Rochester N.Y. (1973), p. 367
64. S.M. Grimes: Ref. 3, Vol. 2, p.95
65. J.B. French and F.K. Ratcliff: Phys. Rev. C3, 94(1971)
66. B. Strohmaier, S.M. Grimes and H. Satyanarayana: Phys. Rev. C36, 1604(1987)
67. A. Gilbert and A.G.W. Cameron: Can. J. Phys. 43, 1446(1965)
68. W. Dilg, W. Schantl, H. Vonach and M. Uhl: Nucl. Phys. A217, 269(1973)
69. T. von Egidy, A.N. Behkami and H.H. Schmidt: Nucl. Phys. A454, 109(1986)
70. W.D. Meyers and W.S. Swiatecki: Ark. Fys. 36, 343(1967)
71. A.V. Ignatyuk, G.N. Smirenkin and A.S. Tishin: Sov. J. Nucl. Phys. 21, 255(1975)
72. A.V. Ignatyuk, K.K. Istekov and G.N. Smirenkin: Sov. J. Nucl. Phys. 29, 450(1979)
73. A.V. Ignatyuk, A.B. Klepatskii, V.M. Maslov and E.Sh. Sukhovitskii: Sov. J. Nucl. Phys. 42, 360(1986)
74. S.K. Kataria, V.S. Ramamurthy and S.S. Kapoor: Phys. Rev. C18, 549(1978)
75. V.S. Ramamurthy, S.K. Kataria and S.S. Kapoor: Proc. of the IAEA Advisory Group Meeting on Basic and Applied Problems of Nuclear Level Density, ed. by M.R. Bhat, Brookhaven, N.Y. (1983), p.187
76. G.E. Mitchell: private communication
77. H. Vonach: private communication
78. A. Mengoni, F. Fabbri and G. Maino: Nuovo Cimento, A94, 297(1986)
79. G. Maino, E. Menapace and A. Ventura: Nuovo Cimento, A57, 427(1980)
80. H.M. Agrawal, J.B. Garg and J.A. Harvey: Phys. Rev. C30, 1880(1984)
81. C. Jacquemin and S.K. Kataria: Z. Physik, A324, 261(1986)
82. S.M. Grimes: Ref. 35
83. E. Sheldon et al.: J. Phys. G: Nucl. Phys. 12, 237 and 446(1986); (b) E. Sheldon and D.W.S. Chan: J. Phys. G: Nucl. Phys. 13, 227(1987)
84. J.Q. Shao et al. Nucl. Sci. Eng. 92, 350(1986)

85. A.V. Ignatyuk, V.P. Lunev, V.G. Pronyaev and E.L. Trykov: Ref. 12a
86. V.A. Madsen, V.R. Brown and J.D. Anderson: Phys. Rev. C12, 1205(1975); (b) V.A. Madsen and V.R. Brown: Phys. Rev. Lett. 52, 176(1984); (c) R.D. Smith, V.R. Brown and V.A. Madsen: Phys. Rev. C33, 847(1986)
87. V.R. Brown and V.A. Madsen: Phys. Rev. C11, 1298(1975)
88. L.F. Hansen, I.D. Proctor, D.W. Heikkinen and V.A. Madsen: Phys. Rev. C25, 189(1982)
89. G. Haouat et al.: Phys. Rev. C30, 1795(1984)
90. J.P. Delaroche: Ref. 1, p.249
91. K. Kumar: Phys. Lett. 29B, 25(1969)
92. A. Arima and F. Iachello: Annu. Rev. Nucl. Part. Sci. 31, 75(1981)
93. K. Kumar, Ch. Lagrange, M. Girod and B. Grammaticos: Phys. Rev. C31, 762(1985)
94. Ch. Lagrange and J.C. Brient: J. Phys. 44, 44(1983)
95. Ch. Lagrange and M. Girod: J. Phys. G: Nucl. Phys. 9, L97(1983)
96. S. Mellema et al.: Phys. Rev. C36, 577(1986)
97. J.P. Delaroche and F.S. Dietrich: Phys. Rev. C35, 942(1986)
98. J. Raynal: Ref.1, p.63
99. P.A. Moldauer: Phys. Rev. C12, 744(1975)
100. E. Gadioli et al.: Z. Phys. A325, 61(1986); (b) E. Gadioli et al.: Phys. Rev. C34, 2065(1986); (c) E. Gadioli, E. Gadioli Erba, P. Guazzoni and L. Zetta: Phys. Rev. C37, 79(1988)
101. W. Smits and R.H. Siemssen: Nucl. Phys. A261, 385(1976)
102. M.G. Mustafa, T. Tamura and T. Udagawa: Phys. Rev. C35, 2077(1987)
103. H. Feshbach, A. Kerman and S. Koonin: Ann. Phys. (N.Y.) 125, 429(1980)
104. T. Tamura, T. Udagawa and H. Lenske: Phys. Rev. C26, 379(1982)
105. R. Bonetti: Proc. Int. Conf. on Fast Neutron Physics, Dubrovnik, Yugoslavia, 1986, eds. D. Miljanic, B. Antolkovic and G. Paic, (Ruder Boskovic Institute, Zagreb), p.2
106. A. Marcinkowski: Ref. 12a; (b) Ref. 35
107. H. Gruppelaar and J.M. Akkermans: Ref. 12a; (b) Ref. 35
108. M. Blann: Ref. 12a
109. M. Blann: Phys. Rev. C17, 1871(1978); (b) E. Gadioli, E. Gadioli Erba and G. Tagliaferri: Phys. Rev. C17, 2238(1978)
110. J.M. Akkermans: Radiat. Eff. 95, 103(1986)
111. J. Bisplinghoff: Phys. Rev. C33, 1569(1986); (b) Ref. 35
112. M. Blann: Ref. 35
113. M. Blann and H.K. Vonach: Phys. Rev. C28, 1475(1983)
114. J. Ernst, W. Friedland and H. Stockhorst: Z. Phys. A328, 333(1987)
115. J.M. Akkermans and H. Gruppelaar: Z. Phys. A300, 345(1981)
116. E.D. Arthur et al.: Ref. 12a
117. M. Blann and J. Bisplinghoff: Z. Phys. A326, 429(1987)
118. Shi Xiangjun, H. Gruppelaar and J.M. Akkermans: Nucl. Phys. A466, 333(1987)
119. P. Obložinský: Phys. Rev. C35, 407(1987)
120. D. Ryckbosch and E. Van Camp: Nucl. Phys. A469, 106(1987)
121. C.Y. Fu: Ref. 35
122. M. Avrigeanu, M. Ivascu and V. Avrigeanu: Z. Phys. A329, 177(1988)
123. S.K. Gupta: Z. Phys. A303, 329(1981)
124. J. Dobeš and E. Běťák: Z. Phys. A310, 329(1983)
125. C. Kalbach: Phys. Rev. C33, 818(1986)
126. C. Kalbach: Ref. 35
127. J.M. Akkermans and H. Gruppelaar: Phys. Lett. 157B, 95(1985)
128. B.A. Remington, M. Blann and G.F. Bertsch: Phys. Rev. C35, 1720(1987)
129. P. Obložinský: Ref. 35
130. C. Kalbach: Z. Phys. A283, 401(1977)
131. A. Iwamoto and K. Harada: Phys. Rev. C26, 1821(1983)
132. K. Sato, A. Iwamoto and K. Harada: Phys. Rev. C28, 1527(1983)
133. L. Milazzo Colli and G.M. Braga Marazzan: Nucl. Phys. A210, 297(1973)
134. W. Scobel, M. Blann and A. Mignerey: Nucl. Phys. A287, 301(1977)
135. A.M. Ferrero et al.: Z. Phys A293, 123(1979)
136. E. Gadioli: Ref. 35
137. J. Bisplinghoff and H. Keuser: Phys. Rev. C35, 821(1987)
138. A.M. Blin et al.: Nucl. Phys. A456, 109(1986)
139. C.Y. Fu: Nucl. Sci. Eng. 86, 344(1984); (b) Nucl. Sci. Eng. 92, 440(1986)
140. A.V. Ignatyuk and Yu.V. Sokolov: Sov. J. Nucl. Phys. 17, 376(1973)
141. C. Kalbach: Nucl. Sci. Eng. 95, 70(1986)
142. M. Herman and G. Reffo: Phys. Rev. C36, 1546(1987)
143. K. Harder et al.: Phys. Rev. C36, 834(1987)
144. I. Kumabe et al.: Phys. Rev. C35, 467(1987); (b) I. Kumabe and Y. Watanabe: Phys. Rev. C36, 543(1987); (c) Y. Watanabe et al.: Phys. Rev. C36, 1325(1987)
145. A. Pavlik and H. Vonach: Physics Data 13-4 (1988)
146. M. Uhl: unpublished
147. S.M. Grimes et al.: Phys. Rev. C19, 2127(1979)
148. A.V. Ignatyuk and V.P. Lunev: Ref. 35
149. H. Kalka, D. Seeliger and F.A. Zhivopistsev: Z. Phys. A329, 331(1988) (b) H. Kalka, M. Toryman and D. Seeliger: Ref. 35
150. G. Mantzouranis, H.A. Weidenmüller and D. Agassi: Z. Phys. A276, 145(1976)
151. C. Costa, H. Gruppelaar and J.M. Akkermans: Phys. Rev. C28, 587(1983)
152. A. Iwamoto and K. Harada: Nucl. Phys. A419, 472(1984)
153. M. Blann, W. Scobel and E. Plechaty: Phys. Rev. C30, 1493(1984)
154. K. Kikuchi and M. Kawai: Nuclear Matter and Nuclear Reactions (North Holland, Amsterdam, 1968)
155. H. Machner: Z. Phys. A327, 175(1987)
156. R. Fischer, M. Uhl and H. Vonach: Phys. Rev. C37, 578(1988)
157. G. Traxler et al.: Nucl. Sci. Eng. 90, 174(1985)
158. C. Kalbach and F. Mann: Phys. Rev. C23, 112(1981)
159. C. Kalbach: Los Alamos National Laboratory Informal Document LA-UR-87-4139(1987)
160. M. Bozoian: Ref. 35
161. M. Uhl: Nucl. Sci. Eng., in press
162. B. Strohmaier, S. Tagesen and H. Vonach: Physics Data 13-2 (1980)
163. D.W. Muir: private communication